Published in final edited form as:
Clin Cancer Res. 2008 August 1; 14(15): 4735–4742. doi:10.1158/1078-0432.CCR-07-4372.

Gene Expression Profiling of Papillary Thyroid Carcinoma Identifies Transcripts Correlated with *BRAF* Mutational Status and Lymph Node Metastasis

Gisele Oler[1,2], **Cléber P. Camacho**[2], **Flávio C. Hojaij**[3], **Pedro Michaluart Jr.**[4], **Gregory J. Riggins**[5], and **Janete M. Cerutti**[1,2]

[1]Division of Genetics, Federal University of São Paulo

[2]Division of Endocrinology, Federal University of São Paulo

[3]Division of Head and Neck Surgery, Federal University of São Paulo

[4]Department of Surgery, University of São Paulo Medical School, São Paulo, SP, Brazil

[5]Department of Neurosurgery, Johns Hopkins University School of Medicine, Baltimore, MD, USA

Abstract

Purpose—To identify papillary thyroid carcinoma (PTC)-associated transcripts, we compared the gene expression profiles of three SAGE libraries generated from thyroid tumors and a normal thyroid tissue.

Experimental Design—Selected transcripts were validated in a panel of 57 thyroid tumors using quantitative PCR (qPCR). An independent set of 71 paraffin-embedded sections was used for validation using immunohistochemistry analysis. To determine if PTC-associated gene expression could predict lymph node involvement, a separate cohort of 130 primary PTC (54 metastatic and 76 non-metastatic) was investigated. The $BRAF^{V600E}$ mutational status was compared to qPCR data, to identify genes that might be regulated by abnormal BRAF—MEK—ERK signaling.

Results—We identified and validated new PTC-associated transcripts. Three genes (*CST6, CXCL14, DHRS3*) are strongly associated with PTC. Immunohistochemistry analysis of CXCL14 confirmed the qPCR data and demonstrated protein expression in PTC epithelial cells. We also observed that *CST6, CXCL14, DHRS3* and *SPP1* were associated with PTC lymph node metastasis, with *CST6, CXCL14 and SPP1* being positively correlated with metastasis, and *DHRS3* expression being negatively correlated. Finally, we found a strong correlation between *CST6* and *CXCL14* expression and $BRAF^{V600E}$ mutational status suggesting that these genes may be induced subsequently to *BRAF* activation and, therefore, may be downstream in the BRAF/MEK/ERK signaling pathway.

Conclusion—*CST6, CXCL14, DHRS3* and *SPP1* may play a role in PTC pathogenesis and progression and are possible molecular targets for PTC therapy.

Keywords

Papillary thyroid carcinoma; *BRAF*; *CST6*; *CXCL14*; *DHRS3*

Requests for reprints: Janete Cerutti, PhD. Genetic Bases of Thyroid Tumor Laboratory Rua Pedro de Toledo 669, 11° andar. Federal University of São Paulo 04039-032, São Paulo, SP, Brazil Phone: +55-11-5081-5233 fax: +55-11-5084-5231 E-mail: cerutti-endo@pesquisa.epm.br.

Introduction

Thyroid cancer is the most common endocrine malignancy, with papillary thyroid carcinoma (PTC) and follicular thyroid carcinoma (FTC) being the most frequent tumor subtypes. Although PTC and FTC arise from the follicular epithelial cells, these tumors differ in biological and clinical behavior. Defining molecular differences and similarities between these subtypes of thyroid tumors could provide insights into their pathogenesis and may help identify new therapeutic approaches.

PTC represents 80% of thyroid cancers, and therefore is the most extensively investigated thyroid tumor. So far the main molecular finding is the activating mutations of *RAS/BRAF* or rearrangement of *RET*, both of which activate the MAPK pathway. These genomic events appear to be mutually exclusive and are the earliest mutations occurring in PTC (1-3). *In vitro* analysis showed that *RET/PTC-RAS-BRAF* induce changes in the expression of an overlapping set of genes (4), while other have suggested that the various alterations in this pathway produce distinct patterns of gene expression (5,6). Despite the importance of the MAPK pathway in PTC, it is likely that there are other mutations and subsequent alterations in gene expression that define this cancer.

The premise of this study is that the identification of novel PTC-associated transcripts, combined with previous molecular data, will lead to a better understanding of the events involved in pathogenesis and progression of PTC. We used Serial Analysis of Gene Expression (SAGE) to identify PTC-associated molecular alterations. SAGE was employed because of its ability to accurately produce comprehensive expression profiles and because we have previously conducted independent in-deep SAGE libraries of PTC, FTC, normal thyroid and FTA (follicular thyroid adenoma) (7,8).

In addition to observing the known transcripts altered in PTC, we identified new transcripts expressed in PTC. We selected five genes (*CST6*, *CXCL14*, *DHRS3*, *BCAN* and *SPP1*), to validate by quantitative PCR (qPCR). Immunohistochemistry was performed to determine the immunolocalization of CXCL14. As most of the transcripts were previously associated with progression of other human cancers, we assessed their expression in a panel of 130 primary metastatic and non-metastatic PTCs. Additionally, to investigate if these genes expression might be activated by BRAF—MEK—ERK—MAPK signaling, we combine the mutational status of *BRAF* gene, the most frequent mutated gene in PTC, with the qPCR expression data of 54 metastatic and 76 non-metastatic PTC to look for associations.

Material and Methods

Tissue samples

A total of 57 thyroid tumours and 14 normal adjacent thyroid tissues were used to find PTC associated transcripts. Samples were obtained from patients undergoing thyroid surgery at Hospital São Paulo, Universidade Federal de São Paulo and Hospital das Clínicas, Universidade Estadual de São Paulo. Tissue specimens were frozen immediately after surgical biopsy and stored at -80°C until use. Final histological classifications were obtained from paraffin-embedded sections and comprised 28 PTCs (15 classical and 13 follicular variant), 17 FTCs and 12 FTAs. For protein analysis, an additional set included paraffin-embedded sections selected from the archives of the Department of Pathology, Federal University of São Paulo. H&E-stained sections were reviewed by a pathologist and included 42 PTCs, 10 FTCs, 19 FTAs and 28 matched-normal thyroid tissues. To evaluate if the candidate genes were associated with tumor progression, a panel of 130 primary PTCs (54 metastatic and 76 non-metastatic) were included in a separated validation group. The study was approved by the Ethics

and Research Committees from both Universities and was conducted in accordance with the Declaration of Helsinki Principles.

Cell lines

Follicular (WRO) and papillary (NPA) thyroid carcinoma cell lines were used in this study (generous gifts of Dr. Alfredo Fusco, University Federico II, Naples, Italy). WRO and NPA were grown in DMEM (Invitrogen Corp., Carlsbad, CA) supplemented with 10% FBS (Invitrogen), 100 units/mL of penicillin and 100 μg/mL streptomycin in a humidified incubator containing 5% CO_2 at 37°C. NPA cell line is known to have a number of specific genetic abnormalities including homozygous BRAF mutation (V600E). WRO has a wild-type *BRAF* (1).

Comparison of papillary and follicular thyroid SAGE libraries

The papillary and follicular SAGE libraries, constructed for previous studies (7,8), were compared for this study using SAGE 2000 software. The full set of tag counts for all thyroid libraries is available for downloading or analysis at the Cancer Genome Anatomy Project SAGE Genie Web site (7)[1]. Pair-wise and Monte-Carlo simulations were used to identify transcripts which were statistically different at *P* value of ≤0.001 and minimum tags account of 5. Transcripts that were over-expressed in the PTC library were assessed in the follicular thyroid adenoma and normal thyroid libraries (7). Genes with large expression differences in PTC library were selected for further validation by quantitative PCR (qPCR) (Table 1).

RNA extraction, cDNA synthesis and quantitative PCR (qPCR)

RNA isolation and cDNA synthesis were performed as previously reported (7). An aliquot of cDNA was used in 20μL PCR reaction containing SYBR Green PCR Master Mix (PE Applied Biosystems, Foster City, CA) and 200 nM of each primer for the target or reference gene. The PCR reaction was performed for 40 cycles of a 4-step program: 94°C for 15 s, annealing temperature for 20 s, 72°C for 20 s, and a fluorescence-read step for 20 s. PCR conditions and primer sequences are described in supplementary Table 1. qPCR reactions were performed in triplicate, the threshold cycle (Ct) was obtained using Applied Biosystem software and was averaged (SD ≤1). Gene expression was normalized using the average of 2-control genes (ribosomal protein S8 and QPC), shown by SAGE to be at equivalent levels in all 4 SAGE libraries. Fold changes were calculated as previously described (7,9).

Immunohistochemical analysis

Immunohistochemistry (IHC) staining was performed in a total of 71 formalin-fixed paraffin-embedded thyroid tumors and adjacent normal tissues, as described (7). Antigen retrieval was performed in 1mM of Tris-HCl (pH 8.0) using a steamer for 15 min. Non-specific protein binding sites were blocked by incubation for 30 min in 1% BSA/PBS. Subsequently, slides were incubated overnight with 5μg/mL of primary monoclonal antibody against human BRAK/CXCL14 (clone 131120; R&D Systems, Inc., Minneapolis, MN). The DAKO cytomation HRP system was used for immunodetection. Sections were incubated with the HRP substrate 3,3′-diaminobenzidine (DAB) (Dako Laboratories), counterstained with 1% hematoxylin, and permanently mounted. All slides were scored in a blind fashion and the immunopositivity was determined as follows: negative when less than 10% of the cells were immunoreactive or immunoreactivity was absent and positive when more than 10% of the cells were immunoreactive.

[1]http://cgap.nci.nih.gov/SAGE

Statistical analysis

To identify PTC-associated transcripts, qPRC data were log-transformed before application of the ANOVA test with Bonferroni adjustment to keep the family-wise error rate at 0.5. IHC was analyzed using χ^2. To identify genes that were statistically different between the metastatic and nonmetastatic group, qPCR data was log-transformed before application of the Student's *t*-test (unpaired). The test for association between *BRAF* and gene expression was performed using a Student's *t*-test (unpaired). The tests of qPCR comparisons were performed using the parametric (Pearson) correlation. $P < 0.05$ was used as the cut-off for statistical significance.

Results

SAGE analysis and selection of PTC-associated transcripts

We sought to identify PTC-associated genes. Comparing the expression profile between PTC and FTC revealed that 1670 transcripts were differentially expressed at a Monte Carlo *P* value of ≤ 0.05. Using a more stringent criterion ($P<0.001$) we generated a list of 548 transcripts. Of these genes, 131 were exclusively expressed in the PTC library by >10-fold and 61 by >15-fold. Transcripts that were over-expressed in PTC by >15-fold (excluding tags matched to unknown transcripts and internal tags) were assessed in the FTA and normal thyroid libraries. The most highly expressed transcripts in PTC, not expressed in FTC and not expressed or is at low levels in FTA and normal thyroid libraries, are described in Table 1.

As expected, our analysis revealed transcripts that were previously identified as over-expressed in PTC but also provided novel information (Table 1). Based on the higher difference on level of expression, five genes *(CST6, CXCL14, BCAN, SPP1* and *DRHS3*) were chosen for transcript level validation by qPCR (Table 1).

Validation of over-expressed genes in PTC by qPCR

A confirmatory qPCR analysis was performed for selected PTC-associated genes in an independent set of samples. Relative expression value (RE) for each gene in each profiled sample is presented as mean of log transformed ratios (Fig 1). Briefly, *CST6* (Cystatin E/M) expression levels were increased in 64% of PTCs, but not expressed in FTAs, most normal thyroid tissues and FTCs (Fig. 1*A*). *CXCL14* (Chemokine (C-X-C motif) ligand 14) and *DHRS3* (Dehydrogenase/reductase (SDR family) member 3) expression was elevated in 68% and 79% of PTCs respectively (Fig. 1*B* and *C*). *CXCL14* and *DHRS3* expression were not observed in normal adjacent thyroid tissues and most of FTAs and FTCs. Even though *BCAN* (Brevican) was expressed in 64% of PTCs, it was expressed in a number of FTAs and FTCs (Fig. 1*D*), suggesting that it is not specifically associated with tumorigenesis of PTC. *SPP1* (Osteopontin), a described *RET/PTC*-induced transcriptional target gene (10), was expressed in about 30% of PTCs (Fig. 1*E*). Interestingly, *SPP1* was found expressed at similar levels in about 24% of FTCs. This is the first analysis of *SPP1* expression in FTCs.

To test whether the difference of expression was significant, the log-transformed RE data was used for statistical analysis. This analysis indicates that *CST6, CXCL14, DHRS3* were differentially expressed between PTC and FTC at significant levels ($P < 0.0001$; ANOVA test with Bonferroni correction). The expression was also considered significant among PTC, normal thyroid tissue and FTA ($P \leq 0.0025$). The results are summarized in Fig. 1. *BCAN* was differentially expressed at significant levels between PTC and normal thyroid tissues ($P = 0.0014$). Although *SPP1* was expressed at higher levels in PTC, it was not considered significant.

Protein Expression

The chemokine CXCL14 has been described as ubiquitously expressed in normal tissues, in inflammatory cells and other stromal cells in multiple cancer types (11-14). In order to confirm the qPCR data and investigate the immunolocalization of CXCL14, IHC analysis was performed in an independent set of 71 thyroid tumors and adjacent normal thyroid. CXCL14 staining was observed in the cytoplasm of tumor epithelial cells in 30 PTCs (71%) while adjacent non-neoplastic cells show no expression of this chemokine (Fig. 2*A*-*D*). In addition, most follicular adenomas and follicular carcinomas were negative for CXCL14 in both tumor cells and normal adjacent tissue (Fig. 2*E* and *F*) (P <0.0001).

Evaluation of CST6, CXCL14, DHRS3 and SPP1 expression in metastatic and nonmetastatic PTC

Because *CST6, CXCL14, DHRS3* and *SPP1* have been previously associated with progression of other tumor subtypes (13,15,16), we sought to investigate whether the expression of these genes could predict lymph node involvement. The expression of these transcripts were assessed in a set of 54 metastatic and 76 non-metastatic PTCs. *CST6* and *CXCL14* tumor expression levels were higher in metastatic than in nonmetastatic PTCs (P <0.0001 and P =0.0037 respectively) (Fig. 3*A* and *B*). Although *DHRS3* was expressed in both groups, its expression was higher in non-metastatic PTC (P=0.0284) (Fig. 3*D*). Even though *SPP1* had a higher expression in metastatic than non-metastatic PTC samples, the difference was significant when we considered only PTCs with >1cm (P = 0.0058) (Fig. 3*C*).

Protein-Protein-Association

To determine possible associations among the PTC over-expressed proteins or to find a pathway association, we used a curated signal transduction pathway resource frequently used to analyze the molecular networks[2]. This human pathway annotation project revealed that these molecules are not involved in any of 20 pathways listed on this resource.

Correlation between the BRAF-V600E mutation and gene expression

The *BRAF* V600E mutation is a common event found in the metastatic and non-metastatic PTC samples used in this study (Oler *et al*., manuscript in preparation). Since targets of this pathway are still unknown, combining expression analysis with *BRAF* status may reveal genes regulated by the RAS—RAF—MEK—ERK—MAPK signal transduction pathway. Interestingly, the expression of *CST6* and *CXCL14* differed significantly between the groups *BRAF*-mutated and *BRA*-Wild type (P <0.0001; Fig. 4*A* and *B*). Moreover, when we examined a possible correlation among the four genes identified as over-expressed in PTC, *CST6* and *CXCL14* correlated (r = .745; P< 0.0001). No additional correlations were found. These findings suggest that *CST6* and *CXCL14* expressions may be induced subsequently to *BRAF* activation, and therefore may be downstream of the BRAF/MEK/ERK signaling pathway.

Based on our findings, we tested the level of expression of CXCL14 in thyroid carcinoma cell lines with known *BRAF* mutation status. The qPCR results showed an approximate 30-fold increased expression of *CXCL14* in NPA (homozygous BRAF mutation) compared to WRO (homozygous wild-type *BRAF*) (Fig. 5).

Discussion

To identify PTC-associated genes, a PTC SAGE library was compared with three SAGE libraries generated from different thyroid tumor subtypes and normal thyroid tissue. SAGE

[2]http://www.netpath.org/

was used because it is a comprehensive and quantitative method for analyzing transcriptomes within a cell population.

Our profiling analysis led to the identification of tags that were most abundant in PTC and were not previously associated with thyroid tumorigenesis process such as *DHRS3, NRGN, NUM, GFAP* and *BCAN*. Moreover, we identified transcripts that were previously described as over-expressed in PTC, such as *CST6, CXCL14, SPP1* and *LGALS3* (4,6,16-18). *CXCL14, DHRS3, BCAN, SPP1* and *CST6*, were chosen for validation. Our qPCR results showed that *CST6, DHRS3* and *CXCL14* were over-expressed in PTC at significant levels comparing to all tumor subtypes. Although *BCAN* was over-expressed in a number of PTCs, it was also expressed in several FTCs and FTA. We then compared the expression of *BCAN* in PTC to normal thyroid tissues and found a significant difference.

CST6, also named cystatin M, is a secreted inhibitor of lysosomal cysteine proteases, similar in class to cathepsin B. Interestingly, *CST6* was first described as a tumor suppressor gene that is epigenetically silenced as a consequence of promoter hypermethylation in metastatic breast cancer cell lines (19-21). Others have found *CST6* markedly elevated in metastatic oropharyngeal squamous carcinoma cell lines and in primary tumor from which these cell lines were originated (15). They suggested that *CST6* expression aids metastasis by blocking intrinsic cathepsin B and rescuing tumor cells from TNF-induced apoptosis (15). Although the role of over-expression of *CST6* in PTC is still unclear, our findings are supported by the fact that *CST6* was previously listed as one of the genes up-regulated in PTC and not expressed in FTC (17,18).

DHRS3, also named *retSDR1*, encodes an enzyme that is involved in the generation of storage forms of retinol. The gene is located in 1p36.1, a region commonly deleted or rearranged in human cancers (22). Although some authors suggest that *DHRS3* is involved in a growth/tumor suppressive pathway, *DHRS3* was found constitutively expressed in breast cancer cell lines that were capable of storage of retinol through esterification (22,23). As predicted by SAGE, *DHRS3* was expressed in normal cells but its expression was higher in PTC. A better understanding of the properties and the physiological role of *DHRS3* in PTC need to be clarified.

CXCL14, also named *BRAK*, is a new CXC chemokine with unknown function and receptor selectivity (24). *CXCL14* was described as constitutively expressed in normal tissues, while it is not expressed in the majority of head and neck squamous cell carcinoma (HNSCC), some cervical squamous cell carcinoma and many established tumor cell lines and human cancers (14,24). It was also demonstrated that *CXCL14* is over-expressed in the inflammatory cells adjacent to the tumors (11,12,14). Recently, *CXCL14* was found as over-expressed in myoepithelial cells of in situ breast carcinoma (13). It was suggested that CXCL14 binds to its receptor on epithelial cells and enhances their proliferation, migration and invasion, and therefore acting as paracrine factor. Although CXCL14 expression was found in myoepithelial cells of in situ breast carcinoma, in invasive breast carcinoma cells the expression of CXCL14 was restricted to the tumor epithelial cells. The authors suggested that during tumor progression a paracrine factor may be converted into an autocrine one due to its up regulation in the tumor epithelial cells (13).

In our study *CXCL14* transcript was markedly higher in PTC than in normal thyroid and thyroid lesions analyzed; this is the first report validating *CXCL14* expression in PTC. Additionally, IHC analysis demonstrated that its expression was specifically found in epithelial cancer cells. Although at this moment we can only guess, CXCL14, similar to other chemokines, is also likely to signal through a G protein-coupled receptor and contribute to progression of PTC.

SPP1, also known as osteopontin, was first described in thyroid as a RET/PTC-induced transcriptional target gene (10). Later, it was demonstrated that *SPP1* is a feature of PTC cells with both *RET/PTC* or BRAF (V600E) mutation (4). The authors showed that *SPP1* prevalence and intensity of staining positively correlated with presence of lymph node metastases and tumor size (>1cm). A low prevalence of *SPP1* over-expression was found in follicular variant of PTC (16).

SPP1 was also significantly over-expressed in a variety of cancers, and recent studies strongly support the crucial role of *SPP1* in tumor progression and metastasis (25). In this study we assessed the expression of *SPP1* using qPCR. Although *SPP1* was over-expressed in PTCs, the difference was not considered significant. Of note, the validation set included not only PTC classical variant not larger than 1 cm but also the follicular variant of PTC where *SPP1* was found to be expressed at lower levels. Interestingly, *SPP1* was found expressed at the same levels in FTC; this is the first analysis of *SPP1* in FTC.

Most of the genes validated here were previously correlated with tumor progression (13,15, 16). In order to determine whether *CST6, DHRS3, CXCL14* and *SPP1* could play a role in determining lymph node involvement, we analyzed their gene expression changes in a second set of samples which included metastatic and non-metastatic PTCs. *CST6* and *CXCL14* were associated with presence of lymph node metastases. *SPP1* expression, however, was associated with presence of lymph node metastasis only for tumors >1cm. *DHRS3* is expressed at lower levels in metastatic PTC than in non-metastatic primary tumors. These findings corroborate with previous important studies, where it was suggested that there is a gene expression pattern associated with metastases that seems to be present in primary tumors and that this molecular program of metastasis is shared by multiple solid tumors (26,27).

A common finding for the majority of PTCs is activation of the RET/RAS/RAF/MEK/ERK pathway, which signals for cell growth, proliferation, and prevents apoptosis, and differentiation (1). Transcriptional profiling of either *in vitro* models or cohort of PTC harboring mutation in one of these oncogenes has produced some contradictory conclusions concerning gene expression altered by this pathway. *In vitro* models demonstrated that *RET/PTC3, HRAS* and *BRAF* induce changes in the expression of a widely overlapping set of genes; it is triggered by up-regulation of several CXC chemokines and their receptors (4). Other found that the mutational status is the principal determinant of the gene expression variation observed within PTC (6). One important aspect that emerged from this last study is the fact that these oncogenes may be able to signal through different pathways and, therefore, activate different targets. Additionally, different proteins may be coupled at different levels to this cascade. Therefore, a more complete understanding of the gene expression induced by the RET-RAS-BRAF-MAPK oncogenic cascade would be useful.

To investigate if there is an association between the presence of *BRAF* mutation and induction of transcripts expression we compared the *BRAF* status in a set of metastatic and non-metastatic PTC with gene expression changes. We found that *CST6* and *CXCL14* over-expression was positively correlated with the *BRAF* V600E mutation in PTC. Our data are in agreement with one of the previously mentioned studies where there is a mutation-specific expression signature that reveals genes with expression altered by the mutation (6). Giordano et al, found 17-fold increased expression of *CST6* and 14-fold increased expression of *CXCL14* (mean expression values) in a set of *BRAF* mutant PTCs compared to *RAS* mutants PTCs (6). Additionally, their expression profile suggested that *BRAF* mutation has a unique role in initiating an immune response in PC and that chemokines such as CXCL14 are involved in the regulation of inflammation status.

Lastly, we also demonstrate that *CXCL14* was over-expressed in a thyroid carcinoma cell line with a homozygous *BRAF* mutation, while its expression was absent in the *BRAF* wild-type WRO. These results are consistent with the induction of *CXCL14* expression by BRAF mutations in PTC.

In this study we identified and validated new genes associated with the etiology of PTC. Indeed, *CST6* and *CXCL14* are associated with the presence of lymph node metastases and *DHRS3* is under-expressed in metastatic PTC. Consequently, these transcripts might be prognostic markers for these tumors, but this hypothesis needs testing. Furthermore, *CST6* and *CXCL14* may be downstream targets of *BRAF* pathway mutational activation.

Supplementary Material

Refer to Web version on PubMed Central for supplementary material.

Acknowledgements

The São Paulo State Research Foundation (FAPESP) from grants 04/15288-0 and 05/60330-8, NIH Grant CA113461, and the Virginia and D.K. Ludwig Fund for Cancer Research. JMC is an investigator of the Brazilian Research Council (CNPq), GO is a scholar from FAPESP and GJR is the recipient of the Irving J. Sherman M.D. Research Professorship.

REFERENCES

1. Kimura ET, Nikiforova MN, Zhu Z, et al. High prevalence of BRAF mutations in thyroid cancer: genetic evidence for constitutive activation of the RET/PTC-RAS-BRAF signaling pathway in papillary thyroid carcinoma. Cancer Res 2003;63:1454–7. [PubMed: 12670889]
2. Soares P, Trovisco V, Rocha AS, et al. BRAF mutations and RET/PTC rearrangements are alternative events in the etiopathogenesis of PTC. Oncogene 2003;22:4578–80. [PubMed: 12881714]
3. Viglietto G, Chiappetta G, Martinez-Tello FJ, et al. RET/PTC oncogene activation is an early event in thyroid carcinogenesis. Oncogene 1995;11:1207–10. [PubMed: 7566982]
4. Melillo RM, Castellone MD, Guarino V, et al. The RET/PTC-RAS-BRAF linear signaling cascade mediates the motile and mitogenic phenotype of thyroid cancer cells. J Clin Invest 2005;115:1068–81. [PubMed: 15761501]
5. Frattini M, Ferrario C, Bressan P, et al. Alternative mutations of BRAF, RET and NTRK1 are associated with similar but distinct gene expression patterns in papillary thyroid cancer. Oncogene 2004;23:7436–40. [PubMed: 15273715]
6. Giordano TJ, Kuick R, Thomas DG, et al. Molecular classification of papillary thyroid carcinoma: distinct BRAF, RAS, and RET/PTC mutation-specific gene expression profiles discovered by DNA microarray analysis. Oncogene 2005;24:6646–56. [PubMed: 16007166]
7. Cerutti JM, Delcelo R, Amadei MJ, et al. A preoperative diagnostic test that distinguishes benign from malignant thyroid carcinoma based on gene expression. J Clin Invest 2004;113:1234–42. [PubMed: 15085203]
8. Cerutti JM, Oler G, Michaluart P Jr. et al. Molecular profiling of matched samples identifies biomarkers of papillary thyroid carcinoma lymph node metastasis. Cancer Res 2007;67:7885–92. [PubMed: 17699795]
9. Cerutti JM, Latini FR, Nakabashi C, et al. Diagnosis of suspicious thyroid nodules using four protein biomarkers. Clin Cancer Res 2006;12:3311–8. [PubMed: 16740752]
10. Castellone MD, Celetti A, Guarino V, et al. Autocrine stimulation by osteopontin plays a pivotal role in the expression of the mitogenic and invasive phenotype of RET/PTC-transformed thyroid cells. Oncogene 2004;23:2188–96. [PubMed: 14981541]
11. Shurin GV, Ferris RL, Tourkova IL, et al. Loss of new chemokine CXCL14 in tumor tissue is associated with low infiltration by dendritic cells (DC), while restoration of human CXCL14 expression in tumor cells causes attraction of DC both in vitro and in vivo. J Immunol 2005;174:5490–8. [PubMed: 15843547]

12. Starnes T, Rasila KK, Robertson MJ, et al. The chemokine CXCL14 (BRAK) stimulates activated NK cell migration: implications for the downregulation of CXCL14 in malignancy. Exp Hematol 2006;34:1101–5. [PubMed: 16863917]
13. Allinen M, Beroukhim R, Cai L, et al. Molecular characterization of the tumor microenvironment in breast cancer. Cancer Cell 2004;6:17–32. [PubMed: 15261139]
14. Frederick MJ, Henderson Y, Xu X, et al. In vivo expression of the novel CXC chemokine BRAK in normal and cancerous human tissue. Am J Pathol 2000;156:1937–50. [PubMed: 10854217]
15. Vigneswaran N, Wu J, Zacharias W. Upregulation of cystatin M during the progression of oropharyngeal squamous cell carcinoma from primary tumor to metastasis. Oral Oncol 2003;39:559–68. [PubMed: 12798398]
16. Guarino V, Faviana P, Salvatore G, et al. Osteopontin is overexpressed in human papillary thyroid carcinomas and enhances thyroid carcinoma cell invasiveness. J Clin Endocrinol Metab 2005;90:5270–8. [PubMed: 15998773]
17. Aldred MA, Huang Y, Liyanarachchi S, et al. Papillary and follicular thyroid carcinomas show distinctly different microarray expression profiles and can be distinguished by a minimum of five genes. J Clin Oncol 2004;22:3531–9. [PubMed: 15337802]
18. Huang Y, Prasad M, Lemon WJ, et al. Gene expression in papillary thyroid carcinoma reveals highly consistent profiles. Proc Natl Acad Sci U S A 2001;98:15044–9. [PubMed: 11752453]
19. Sotiropoulou G, Anisowicz A, Sager R. Identification, cloning, and characterization of cystatin M, a novel cysteine proteinase inhibitor, down-regulated in breast cancer. J Biol Chem 1997;272:903–10. [PubMed: 8995380]
20. Zhang J, Shridhar R, Dai Q, et al. Cystatin m: a novel candidate tumor suppressor gene for breast cancer. Cancer Res 2004;64:6957–64. [PubMed: 15466187]
21. Rivenbark AG, Jones WD, Coleman WB. DNA methylation-dependent silencing of CST6 in human breast cancer cell lines. Lab Invest 2006;86:1233–42. [PubMed: 17043665]
22. Cerignoli F, Guo X, Cardinali B, et al. retSDR1, a short-chain retinol dehydrogenase/reductase, is retinoic acid-inducible and frequently deleted in human neuroblastoma cell lines. Cancer Res 2002;62:1196–204. [PubMed: 11861404]
23. Haeseleer F, Huang J, Lebioda L, Saari JC, Palczewski K. Molecular characterization of a novel short-chain dehydrogenase/reductase that reduces all-trans-retinal. J Biol Chem 1998;273:21790–9. [PubMed: 9705317]
24. Hromas R, Broxmeyer HE, Kim C, et al. Cloning of BRAK, a novel divergent CXC chemokine preferentially expressed in normal versus malignant cells. Biochem Biophys Res Commun 1999;255:703–6. [PubMed: 10049774]
25. Rangaswami H, Bulbule A, Kundu GC. Osteopontin: role in cell signaling and cancer progression. Trends Cell Biol 2006;16:79–87. [PubMed: 16406521]
26. van ’t Veer LJ, Dai H, van de Vijver MJ, et al. Gene expression profiling predicts clinical outcome of breast cancer. Nature 2002;415:530–6. [PubMed: 11823860]
27. Ramaswamy S, Ross KN, Lander ES, Golub TR. A molecular signature of metastasis in primary solid tumors. Nat Genet 2003;33:49–54. [PubMed: 12469122]

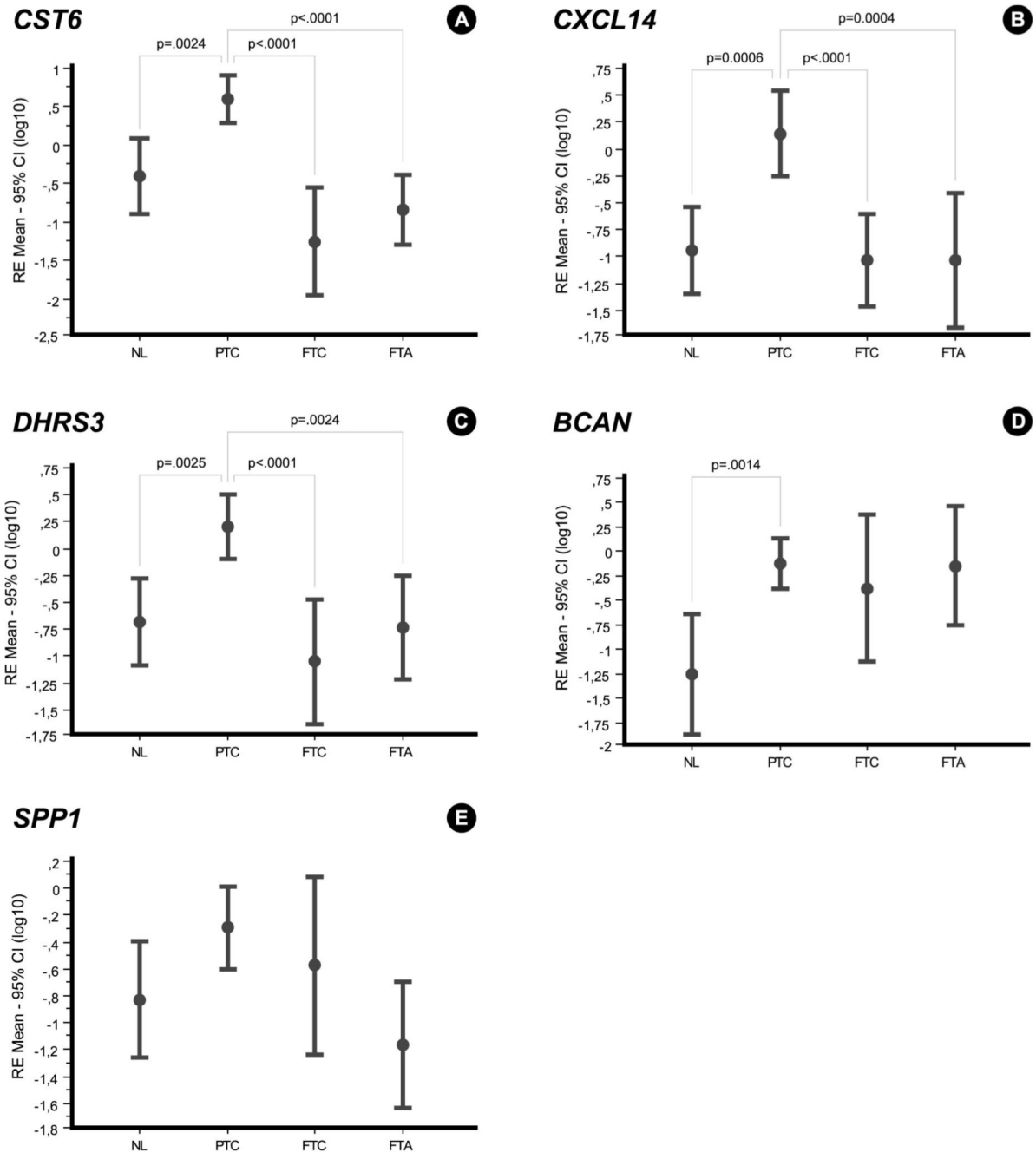

Figure 1.

Relative expression levels (RE) of selected transcripts in 71 thyroid samples as determined by qPCR. Tissue histology consists of 28 PTCs (15 classical and 13 follicular variant), 17 FTCs, 12 FTAs and 14 normal adjacent tissues. Transcripts were normalized to the average of two control genes (QPC and S8) and RE was calculated as described in material and methods. The RE data were log transformed before the application of statistical test (ANOVA with Bonferroni correction). The results are presented as mean of log transformed data with 95% CI (confidence interval). Significant differences were observed to *CST6*, *CXCL14*, *DHRS3* and *BCAN*.

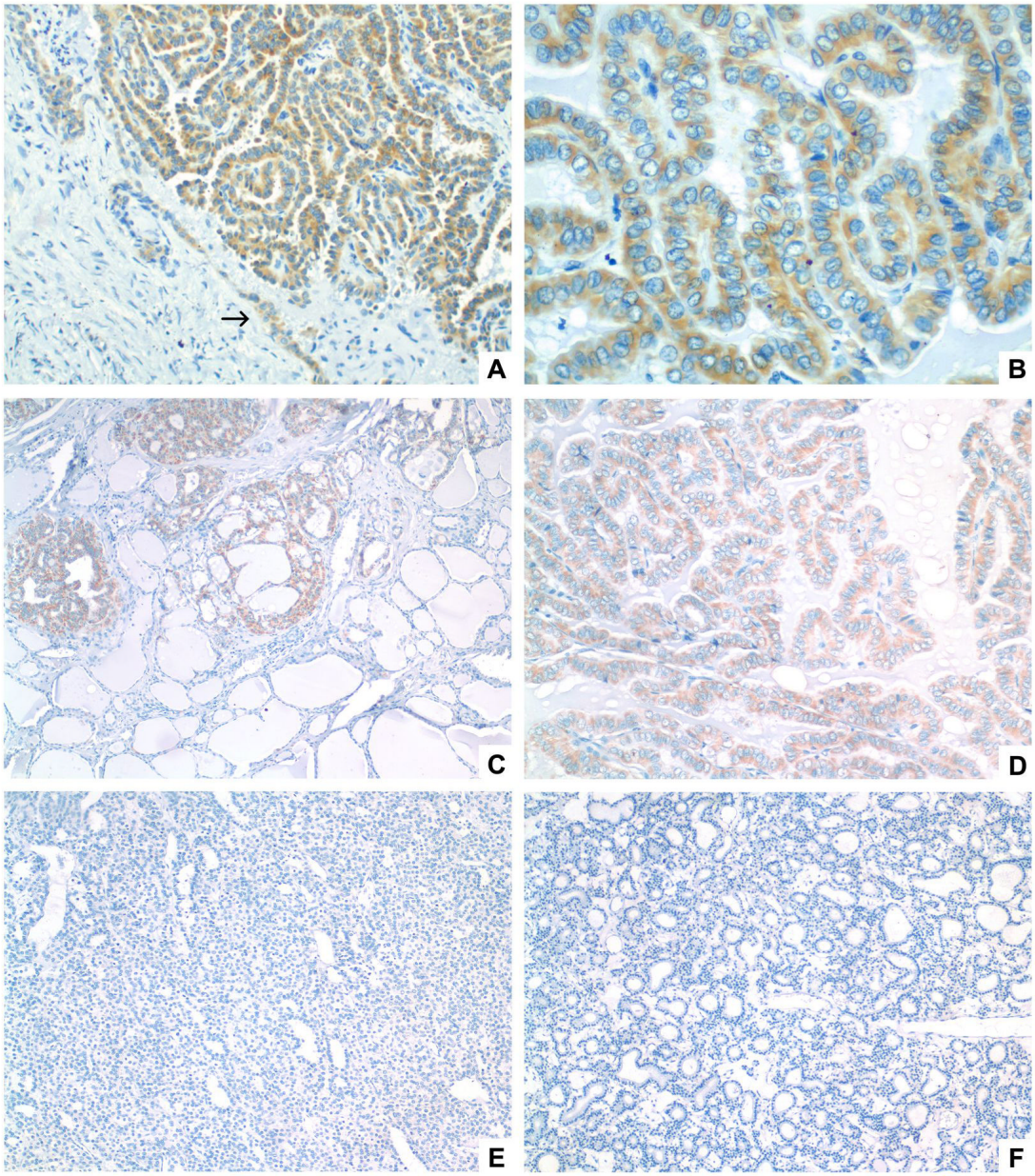

Figure 2.
Immunohistochemical analysis of CXCL14 in paraffin-embedded sections of thyroid tumors. *A-D*, PTCs exhibited a strong staining in epithelial cancer cells while no staining was observed in non-tumoral tissues. *E-D*, FTC and FTA respectively exhibited no immunoreactivity. The arrow in PTC shows negative staining in stromal cells and normal adjacent follicular cells. Original magnification is x 100 (*C*, *E* and *F*), x 200 (*A* and *D*) and x 400 (*B*).

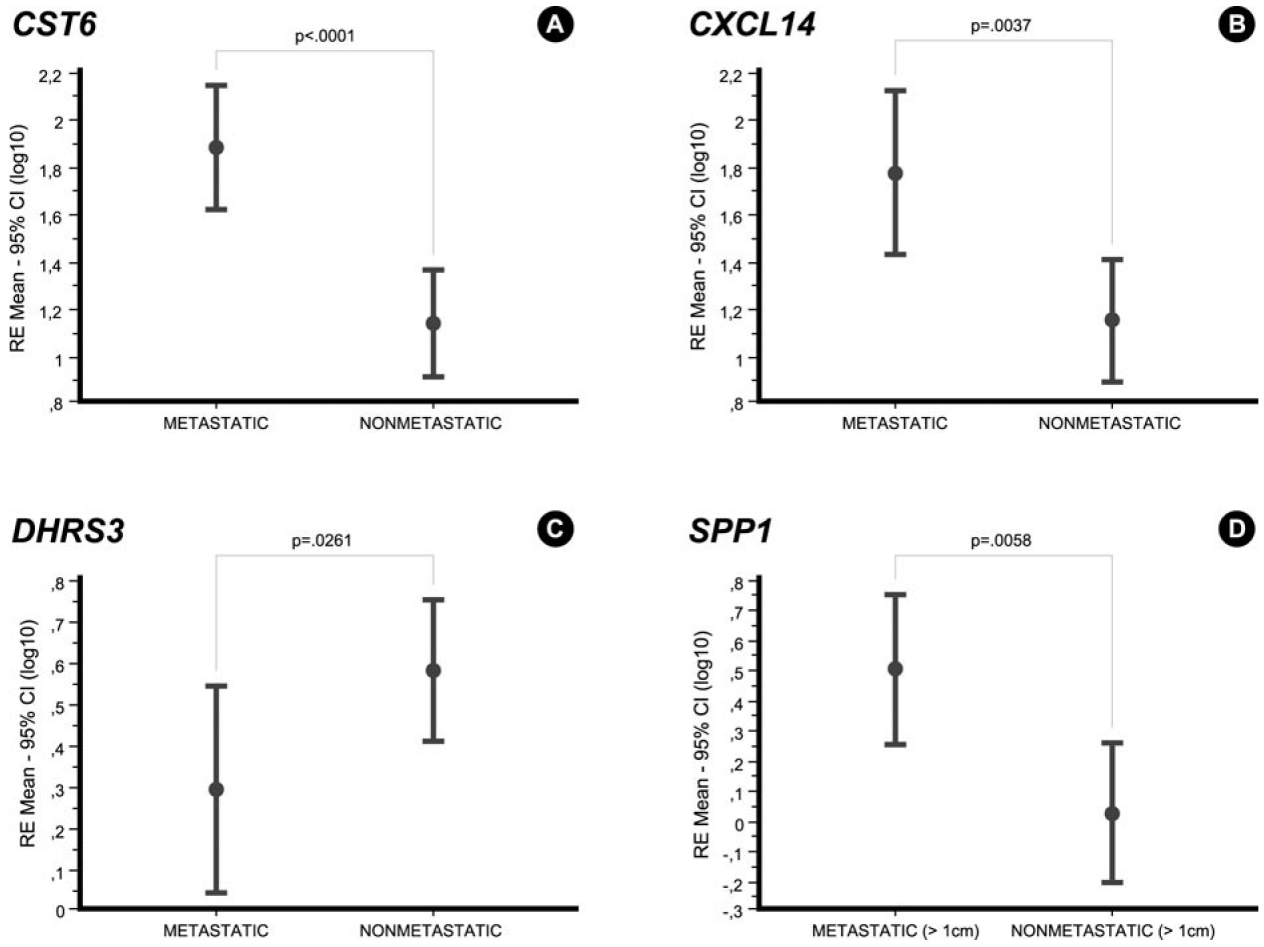

Figure 3.

Relative expression levels (RE) determined by qPCR in 76 samples of nonmetastatic and 54 metastatic primary PTCs. Transcripts were normalized to the average of two control genes (QPC and S8) and RE was calculated as described in material and methods. The RE values were log transformed before the application of statistical analysis (Student's *t*-test). The results are presented as mean of log transformed data with 95% CI (confidence interval).

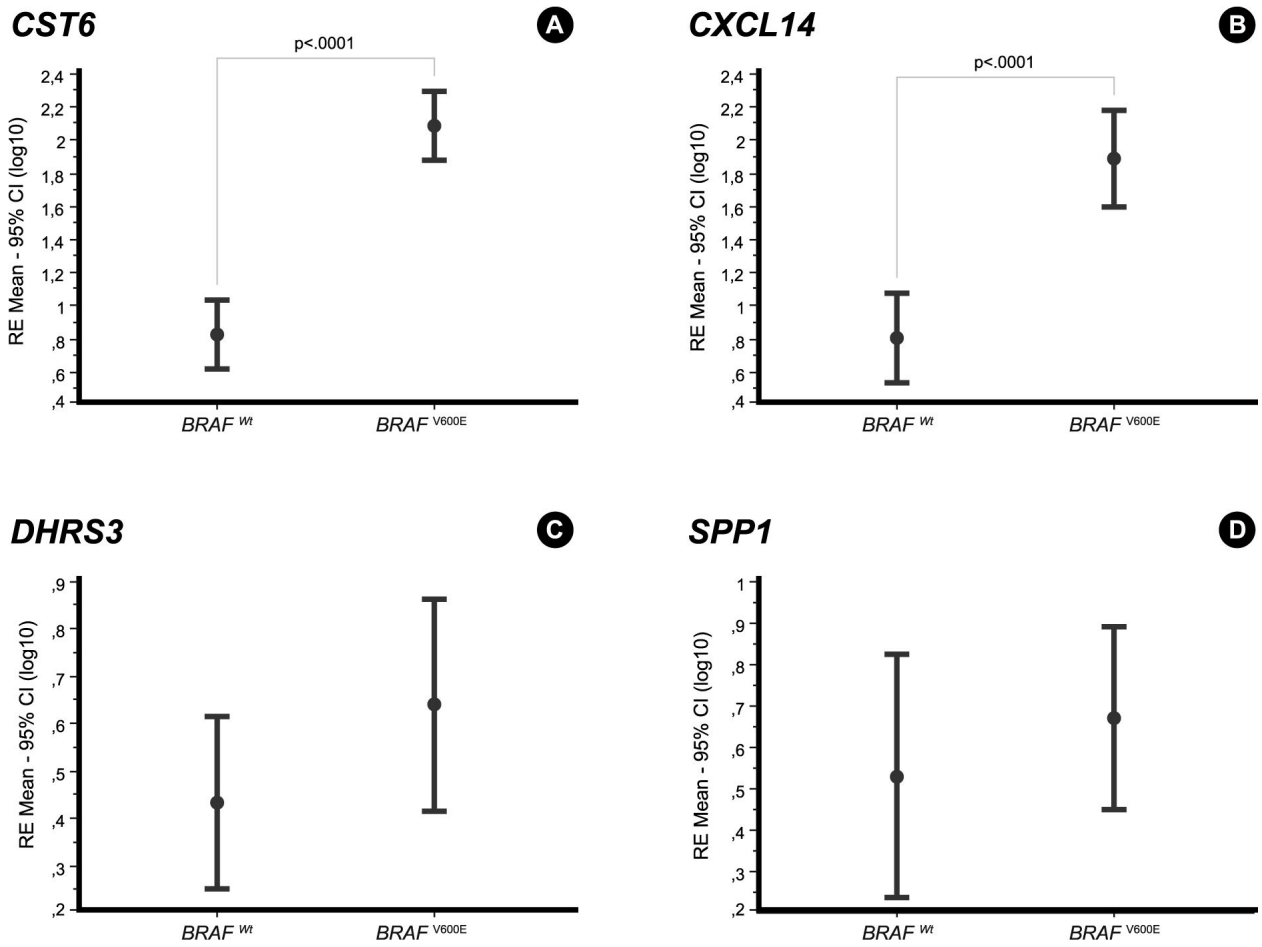

Figure 4.

BRAF status and qPCR analysis in metastatic and non-metastatic PTCs. RE- Relative expression levels determined by qPCR were calculated as described in figure 3. Association between *BRAF* status and gene expression was calculated using Student's *t*-test. *CST6* and *CXCL14* were associated with the presence of BRAF ^{V600E} mutation.

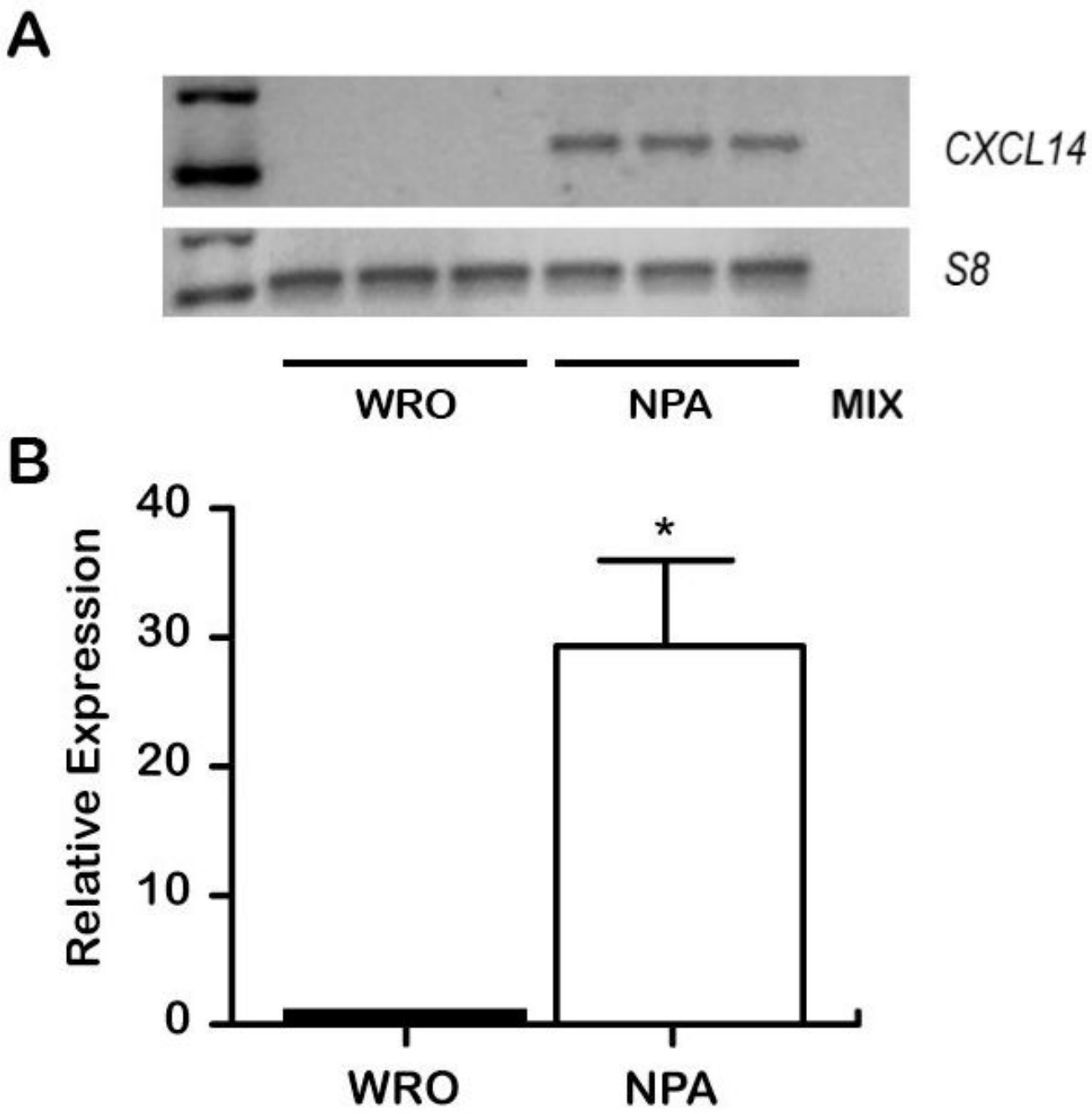

Figure 5.

Representative results from qPCR analysis in NPA and WRO thyroid carcinoma cell lines. A) qPCR products were visualized on an agarose gel. Each experiment was performed in triplicate. Transcripts were normalized to the average of S8 and RE was calculated as described in material and methods. B) The RE values were log transformed before the application of statistical analysis (Student's *t*-test; *P*=0.0047). The results are presented as mean of the two triplicates from two independent experiments.

Table 1

Transcripts differentially expressed in PTC library compared with FTC, FTA and normal libraries.

SAGE Tags	NL*	PTC*	FTC*	FTA*	Gene Symbol	Transcript Description$^{\theta}$	GenBank acession no.
GTGGAGGGCA	10	250	0	0	***CST6***$^{\psi}$	Cystatin E/M	NM_001323
CAGGTTTCAT	1	89	0	0	***CXCL14***$^{\psi}$	Chemokine (C-X-C motif) ligand 14	NM_004887
ACGAGGGGTG	0	20	0	0	***BCAN***$^{\psi}$	Brevican	NM_198427
AATAGAAATT	0	19	0	1	***SPP1***$^{\psi}$	Secreted phosphoprotein 1 (osteopontin)	NM_000582
CTTCTGCTGG	6	30	0	8	***DHRS3***$^{\psi}$	Dehydrogenase/reductase (SDR family) member 3	NM_004753
ATATAATCTG	5	43	0	8	***LGALS3***	Lectin, galactoside-binding, soluble, 3 (galectin 3)	NM_194327
ACTTTGTCCC	0	19	0	0	***GFAP***	Glial fibrillary acidic protein	NM_002055
CCTGCCCCGC	1	48	0	0	***SLC34A2***	Solute carrier family 34 (sodium phosphate), member 2	NM_006424
AGAGAAGAAT	0	36	0	0	***NMU***	Neuromedin U	NM_006681
TGACTGTGCT	5	29	0	0	***NRGN***	Neurogranin (protein kinase C) substrate, RC3)	NM_006176

*SAGE tags counts shown in each column refer to the number of SAGE tags in the libraries after normalization to 200,000 total tags.

$^{\theta}$Transcript description refers to the gene name to which tag was attributed, according to the HUGO/GDB nomenclature committee approved symbols.

$^{\psi}$Transcripts selected for validation by qPCR.